Inorganic Chemistry

Article

pubs.acs.org/IC

The Effect of Specific Solvent–Solute Interactions on Complexation of Alkali-Metal Cations by a Lower-Rim Calix[4]arene Amide Derivative

Gordan Horvat,[†] Vladimir Stilinović,[†] Branko Kaitner,[†] Leo Frkanec,[‡] and Vladislav Tomišić*[,†]

[†]Department of Chemistry, Faculty of Science, University of Zagreb, Horvatovac 102a, 10000, Zagreb, Croatia

[‡]Laboratory of Supramolecular and Nucleoside Chemistry, Department of Organic Chemistry and Biochemistry, Ruđer Bošković Institute, Bijenička c. 54, 10000, Zagreb, Croatia

Supporting Information

ABSTRACT: Complexation of alkali-metal cations with calix[4]arene secondary-amide derivative, 5,11,17,23-tetra(*tert*-butyl)-25,26,27,28-tetra(*N*-hexylcarbamoylmethoxy)calix[4]arene (**L**), in benzonitrile (PhCN) and methanol (MeOH) was studied by means of microcalorimetry, UV and NMR spectroscopies, and in the solid state by X-ray crystallography. The inclusion of solvent molecules (including acetonitrile, MeCN) in the calixarene hydrophobic cavity was also investigated. The classical molecular dynamics (MD) simulations of the systems studied were carried out. By combining the results obtained using the mentioned experimental and computational techniques, an attempt was made to get an as detailed insight into the complexation reactions as possible. The thermodynamic parameters, that is, equilibrium constants, reaction Gibbs energies, enthalpies, and entropies, of the investigated processes were determined and discussed. The stability constants of the 1:1 (metal:ligand) complexes measured by different methods were in very good agreement. Solution Gibbs energies of the ligand and its complexes with Na^+ and K^+ in methanol and acetonitrile were determined. It was established that from the thermodynamic point of view, apart from cation solvation, the most important reason for the huge difference in the stability of these complexes in the two solvents lay in the fact that the transfer of complex species from MeOH to MeCN was quite favorable. That could be at least partly explained by a more exergonic inclusion of the solvent molecule in the complexed calixarene cone in MeCN as compared to MeOH, which was supported by MD simulations. Molecular and crystal structures of the lithium cation complex of **L** with the benzonitrile molecule bound in the hydrophobic calixarene cavity were determined by single-crystal X-ray diffraction. As far as we are aware, for the first time the alkali-metal cation was found to be coordinated by the solvent nitrile group in a calixarene adduct. According to the results of MD simulations, the probability of such orientation of the benzonitrile molecule included in the ligand cone was by far the largest in the case of LiL^+ complex. Because of the favorable PhCN–Li^+ interaction, **L** was proven to have the highest affinity toward the lithium ion in benzonitrile, which was not the case in the other solvents examined (in acetonitrile, sodium complex was the most stable, whereas in methanol, complexation of lithium was not even observed). That could serve as a remarkable example showing the importance of specific solvent–solute interactions in determining the equilibrium in solution.

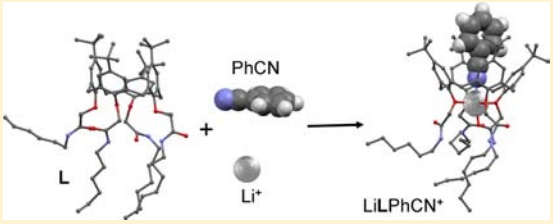

INTRODUCTION

Calixarene derivatives have been well-known as versatile binders of cations, anions, and neutral molecules.[1] The binding abilities of these macrocyclic compounds toward different species can be rather easily tuned by introducing the appropriate substituents at their lower and/or upper rim. The lower-rim derivatives comprising carbonyl functional groups, that is, ketones, esters, and amides, have been extensively studied and shown to form quite stable complexes with alkali-, alkaline-earth, and transition-metal cations in various solvents.[2] The receptor affinity toward particular cation is affected by several factors, the most important being the nature of the substituents on phenolic oxygen atoms forming the cation-binding site, and the compatibility of the size of this site with that of the metal ion. In addition, the binding process is often strongly influenced by the solvation of the reactants and the complex(es) formed.[1d,3] In this respect, the specific solvent–ligand and solvent–complex interactions, that is, inclusion of the solvent molecule in a calixarene hydrophobic cavity, can play a very important role in determining the complexation equilibrium.[3a,b,4]

In the calixarene derivatives bearing substituents with secondary-amide groups, both a hydrogen-bond acceptor (carbonyl group) and a hydrogen-bond donor (–NH– group) are present, and consequently intramolecular NH···O=C H-bonds can be formed. These bonds need to be

Received: July 24, 2013
Published: October 21, 2013

   dx.doi.org/10.1021/ic4019184 | *Inorg. Chem.* 2013, 52, 12702–12712

disrupted upon cation complexation, and that can produce a remarkable effect on the macrocycle binding abilities.[3b,4a,5]

Recently, we have reported on a thorough study of the complexation of alkali-metal cations by a lower-rim secondary amide calix[4]arene derivative, 5,11,17,23-tetra(*tert*-butyl)-25,26,27,28-tetra(*N*-hexylcarbamoylmethoxy)calix[4]arene (**L**, Figure 1), in acetonitrile.[4a] This Article is focused on detailed

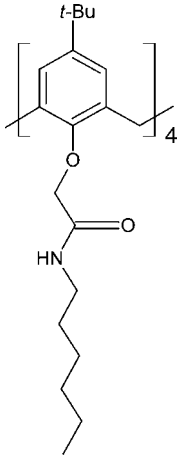

Figure 1. Structure of **L**.

thermodynamic, structural, and computational investigations of the solvent (benzonitrile, PhCN; methanol, MeOH; acetonitrile, MeCN) effect on the complexation reactions of **L**. For that reason, microcalorimetry, UV and NMR spectroscopies, single-crystal X-ray diffraction, and classical molecular dynamics (MD) computations were employed. The solvation of cations, ligand, and complexes was addressed, with particular emphasis on the above-mentioned specific interactions of solvent molecules with the free and complexed ligand in solution and in the solid state. In line with this, a solid-state structure of the ternary Li**L**PhCN$^+$ complex was determined in which the lithium cation was coordinated by a nitrile nitrogen atom of the benzonitrile molecule included in the calixarene hydrophobic cone. To the best of our knowledge, such coordination of an alkali-metal cation in the calixarene complex was seen for the first time. The finding was supported by MD simulations. In addition, it was found that coordination of the lithium cation by the solvent molecule was closely related to the observed selectivity of **L** in solution. The influence of intramolecular hydrogen bonds on the complex stabilities was discussed as well.

EXPERIMENTAL SECTION

Materials. Compound **L** was prepared according to the procedure described elsewhere.[4a] The solvents, acetonitrile (MeCN, Merck, Uvasol and J. T. Baker, HPLC grade), benzonitrile (Sigma Aldrich, Chromasolv, 99.9%), and methanol (J. T. Baker, HPLC grade) were used without further purification. The salts used for the investigation of **L** complexation were $LiClO_4$ (Sigma Aldrich, 99.99%), LiCl (Fluka, 99%), $NaClO_4$ (Sigma Aldrich, 98+%), $KClO_4$ (Merck, p.a.), KCl (Merck, p.a.), RbCl (Sigma, 99%), and CsCl (Sigma, 99.5%).

Solubility Measurements. Saturated solutions of **L** in acetonitrile and methanol were prepared by adding an excess amount of the solid substance to the solvent. The obtained mixtures were left in a thermostat at 25 °C for several days to equilibrate. The concentrations of saturated **L** solutions were determined at 25.0 °C spectrophotometrically by means of a Varian Cary 5 spectrophotometer equipped with a thermostatting device. Calibration curves were obtained by measuring the absorbances of **L** solutions of known concentrations.

Spectrophotometry. UV titrations of **L** with alkali-metal salt solutions in methanol were performed at (25.0 ± 0.1) °C by means of a Varian Cary 5 spectrophotometer. The metal salt solution (c = 3.25 × 10^{-4}–0.141 mol dm^{-3}) was added to a ligand solution (V_0 = 2.0–2.5 cm^3, c_0 = 4.40 × 10^{-4}–7.11 × 10^{-4} mol dm^{-3}) placed in the quartz cell (l = 1 cm). After each addition, the UV spectrum was recorded with a sampling interval of 1 nm and integration time of 0.2 s. All measurements were done in triplicate. The obtained data were analyzed by multivariate nonlinear regression analysis using the SPECFIT program.[6]

^{1}H NMR Studies. ^{1}H NMR titrations were carried out at 25 °C by means of a Bruker Avance 600 MHz with a solvent signal used as standard for titrations in CD_3OD or with a TMS signal as standard in $CDCl_3$ solutions. In titration of **L** with the sodium cation in methanol, the solution made of $NaClO_4$ (c = 3.84 × 10^{-2} mol dm^{-3}) and **L** (c = 9.72 × 10^{-4} mol dm^{-3}) was added to the CD_3OD solution of **L** (c = 9.72 × 10^{-4} mol dm^{-3}). Titrations of **L** and [Na**L**]ClO_4 with methanol in $CDCl_3$ were performed by the addition of MeOH solution in deuterated chloroform (c = 0.411 mol dm^{-3}) to the solution of the ligand (c = 4.65 × 10^{-3} mol dm^{-3}) and the complex (c = 4.08 × 10^{-2} mol dm^{-3}), respectively. Spectra were recorded at 32 pulses. The equilibrium constants determined from ^{1}H NMR titration data were computed by HypNMR program.[7]

Calorimetry. Microcalorimetric measurements were conducted with an isothermal titration calorimeter Microcal VP-ITC at 25.0 °C. The calorimeter was calibrated electrically, and its reliability was additionally checked by carrying out the complexation of barium(II) by 18-crown-6 in aqueous medium at 25 °C. The results obtained (log K = 3.75, $\Delta_r H$ = −31.7 kJ mol^{-1}) were in excellent agreement with the literature values (log K = 3.73, $\Delta_r H$ = −31.5 kJ mol^{-1}).[8] Thermograms were processed using the Microcal OriginPro 7.0 program.

In the calorimetric studies of alkali-metal complexation by **L**, the enthalpy changes were recorded upon stepwise additions of benzonitrile or methanol solution of metal salt into solution of ligand (V_0 = 1.4182 cm^3). Titrations of the Li^+–**L** and Na^+–**L** complexes with acetonitrile in benzonitrile were carried out by the addition of MeCN solution in PhCN to the solution of complexes in the same solvent. The heats measured in the titration experiments were corrected for heats of titrant dilution obtained by blank experiments. The dependence of successive enthalpy changes on the titrant volume was processed by nonlinear least-squares fitting procedure using the OriginPro 7.5 program. All measurements were repeated three or more times.

X-ray Structure Determination. Single crystals of [Li**L**]ClO_4–PhCN were obtained by slow evaporation of an equimolar benzonitrile solution of $LiClO_4$ and **L**.

The crystal and molecular structures were determined by single-crystal X-ray diffraction. Diffraction measurements were made on an Oxford Diffraction Xcalibur Kappa CCD X-ray diffractometer with graphite-monochromated Mo K_α (λ = 0.71073 Å) radiation.[9] The data sets were collected using the ω scan mode over the 2θ range up to 54°. The structures were solved by direct methods and refined using SHELXS and SHELXL programs.[10] The structural refinement was performed on F^2 using all data. The hydrogen atoms were placed in calculated positions and treated as riding on their parent atoms [C–H = 0.93 Å and U_{iso}(H) = 1.2 U_{eq}(C); C–H = 0.97 Å and U_{iso}(H) = 1.2 U_{eq}(C)]. All calculations were performed and drawings prepared using the WinGX crystallographic suite of programs.[11]

Crystal data: $C_{83}H_{121}ClLiN_5O_{12}$, M_r = 1423.24, space group $C2/c$, a = 31.569(2) Å, b = 15.806(9) Å, c = 35.945(3) Å, β = 105.781(7)°, V = 17260(10) $Å^3$, Z = 8, ρ = 1.095 g cm^{-3}, μ = 0.102 mm^{-1}, T = 150 K, crystal dimensions 0.21 × 0.19 × 0.09 mm^3, total of 33 490 collected reflections, 14 497 unique reflections, 5779 observed reflections [$I > 2\sigma(I)$], 974 refined parameters, $\Delta\rho_{max}$ = 1.407 e $Å^{-3}$, $\Delta\rho_{min}$ = −1.151 e $Å^{-3}$, R_1(obs) = 0.1419, wR_2(all) = 0.4099. CCDC 949221 contains the supplementary crystallographic data for this Article. These data can be obtained free of charge from The Cambridge Crystallographic Data Centre via www.ccdc.cam.ac.uk/data_request/cif.

dx.doi.org/10.1021/ic4019184 | *Inorg. Chem.* 2013, 52, 12702–12712

A number of problems were encountered during the structure refinement due to severe disorder of the hexyl chains and, to a minor degree, *tert*-butyl groups and the perchlorate anion. The electron density of the parts of the structure comprising hexyl chains was found to be almost continuous, with few discernible maxima, which would correspond to atom locations. The modeling of the hexyl groups was thus achieved only with numerous restraints of bond distances and angles as well as thermal parameters. Attempts to further model the disorder of the hexyl groups have been abandoned, as the data quality could not justify such an increase in number of refinable parameters, and also as no reasonable positions of atoms could be located in the electron difference map. Having thus modeled hexyl chains, the model was left with several "voids" between symmetry related molecules, which are in reality occupied by disordered hexyl chains. To account for the residual disordered electron density, the SQUEEZE procedure in PLATON was employed.[12] After two cycles of the SQUEEZE procedure and least-squares refinement, convergence was reached. The total number of electrons in the regions occupied by the disordered hexyl chains (1604 Å^3 per unit cell) was estimated as 246 electrons, calculated by SQUEEZE, which corresponded to approximately 30 carbon atoms and hydrogen atoms bound to them. Fortunately, disorder of the hexyl and *tert*-butyl groups did not affect the calixarene cone and the coordination polyhedron, and this part of the structure was successfully modeled with no geometric or other restraints.

Molecular Dynamics Simulations. The molecular dynamics simulations were carried out by means of the GROMACS[13] package (version 4.5.3). Intramolecular and nonbonded intermolecular interactions were modeled by the OPLS-AA (Optimized Parameters for Liquid Simulations-All Atoms) force field.[14] Partial charges assigned to ring carbons bound to CH_2 groups that link the monomers were assumed to be zero. In all simulations, the initial molecular structure of **L** was the one obtained from the Na**L**$^+$ crystal.[4a] The **L**, M**L**$^+$, and corresponding acetonitrile adducts were solvated in a cubical box (edge length 72.6 Å) of benzonitrile with about 2150 molecules, and with periodic boundary conditions. The solute concentration in such a box was about 5×10^{-3} mol dm^{-3}. The solvent box was equilibrated prior to inclusion of **L** and its complexes with the box density after equilibration being close to the experimental one within 2%. The simulations of the aforementioned chemical species in methanol were also conducted. Solutes were solvated in a cubical box (edge length 58.5 Å) of methanol with about 2710 molecules. The solute concentration in these systems was about 0.01 mol dm^{-3}. During the simulations of the systems comprising calixarene and metal cations, Cl^- ion was included to neutralize the box. The chloride counterion was kept fixed at the box periphery, whereas the complex was initially positioned at the box center. In all simulations, an energy minimization procedure was performed followed by a molecular dynamics simulation in *NpT* conditions for 50.5 ns, where the first 0.5 ns was not used in data analysis. The Verlet algorithm[15] with a time step of 1 fs was employed. The cutoff radius for nonbonded van der Waals and short-range Coulomb interactions was 16 Å. Long-range Coulomb interactions were treated by the Ewald method as implemented in the PME (Particle Mesh Ewald) procedure.[16] The simulation temperature was kept at 298.15 K with the Nosé–Hoover[17] algorithm using a time constant of 1 ps. The pressure was kept at 1 bar by the Martyna–Tuckerman–Tobias–Klein[18] algorithm and the time constant of 1 ps. Pictures of calixarene molecular structures were created using VMD software.[19]

RESULTS AND DISCUSSION

Crystal Structure and Stereochemistry of [LiL]ClO_4–PhCN. The coordination polyhedron about the lithium ion is a distorted octahedron. The five shortest bonds of the coordination polyhedron (1.95–2.24 Å) are those between the lithium ion and oxygen atoms of **L**. The lithium ion is placed in the plane of four ether oxygen atoms (it deviates from the mean plane of the atoms by 0.002(3) Å), and is coordinated in the fifth position by one of the amide carboxyl oxygen atoms of **L**. The sixth coordination position is occupied by a nitrogen atom of the benzonitrile molecule, which is positioned within the calixarene cone. This bond of 2.323(12) Å is somewhat longer than the other bonds of the coordination polyhedron, and substantially longer than the average lithium–(nitrile)-nitrogen bond distance (2.05(4) Å) observed in the crystal structures.[20] Although no cases of similar coordination behavior of benzonitrile in the solid state have been reported to date, similar coordination of acetonitrile can be seen in a number of structures of coordination compounds of transition metals with calix[4]arenes. In all of those cases, the acetonitrile molecule is captured within the calixarene cone and acts as a ligand to the central ion. Although in these structures the central cations are substantially larger than lithium (14 structures of Mo complexes, 5 of Cr, 4 of W, 3 of V, 2 of Cd, and 1 of Tl, Figure S1, Supporting Information), the mean M–N distance (2.24(2) Å)[20] is shorter than the Li–N distance in [Li**L**]ClO_4–PhCN, probably due to the sterically hindered inclusion of benzonitrile, as opposed to acetonitrile. The other solvents, such as tetrahydrofurane and pyridine, were also found to enter the calixarene cone, while coordinating metal ions in polynuclear calix[4]arene complexes.[21]

The calixarene cone is of approximate C_4 symmetry with the values of torsion angles about the methylene group bonds being similar to those in the sodium complex of exact C_4 symmetry,[4a] φ between 74° and 89° (82.4° in Na**L**$^+$) and χ between −76° and −88° (74.5° in Na**L**$^+$; for definitions of φ and χ, see ref 22). The cone geometry is somewhat distorted from C_4 symmetry to accommodate the phenyl ring of the benzonitrile molecule. The benzonitrile phenyl ring is placed in the calixarene cone so that it forms two C–H···π hydrogen bonds with two rings of the macrocycle (C82–H82···C27 of 3.800(11) Å and C78–H78···C4 of 3.669(9) Å, Figure 2a),

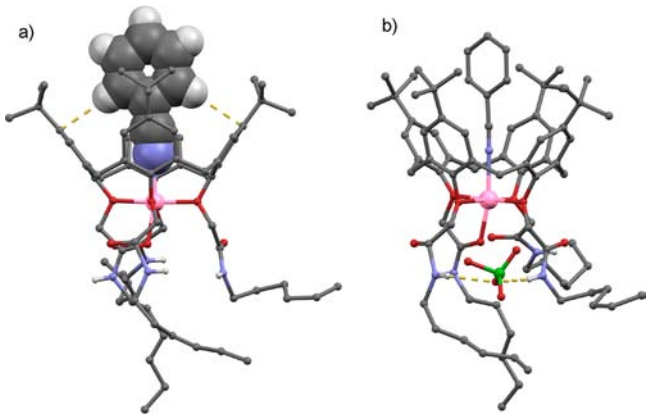

Figure 2. (a) Molecular structure of [Li**L**PhCN]$^+$ showing the intramolecular C–H···π hydrogen bonds between the benzonitrile and calixarene cone phenyl rings. All C-bound hydrogen atoms apart from those on benzonitrile moiety have been omitted for clarity. (b) An [Li**L**PhCN]$^+$[ClO_4]$^-$ ion pair showing hydrogen bonding between the ions. All C-bound hydrogen atoms have been omitted for clarity.

which, in addition to the coordination interaction of the benzonitrile nitrogen atom with the lithium ion, stabilize the [Li**L**PhCN]$^+$ complex. The C–H···π hydrogen bonds also direct the orientation of the phenyl ring so that it is approximately perpendicular (85.6° and 86.9°) to the calixarene phenyl rings with which it interacts, and approximately parallel to the other two (21.6° and 21.5°; the benzonitrile plane

dx.doi.org/10.1021/ic4019184 | *Inorg. Chem.* 2013, 52, 12702–12712

approximately bisects the angle between the two calixarene phenyl ring planes of 42.1°). Thus, the insertion of the benzonitrile molecule into the calixarene hydrophobic basket leads to its slight elongation in the direction parallel to the benzonitrile phenyl ring plane, which can be seen from the angles between the macrocycle plane (defined as the mean plane of the four methylene carbon atoms) and two calixarene cone phenyl rings, which are somewhat larger for the rings (approximately) parallel to the benzonitrile plane (69.6° and 68.3°) than for those (approximately) perpendicular to it (56.4° and 54.9°).

The crystal structure of [Li**L**]ClO_4−PhCN can be described as hydrogen-bonded chains of $[LiLPhCN]^+[ClO_4]^-$ ion pairs. The perchlorate ion is caught in a hydrogen-bond pincer formed by two N−H groups of the calixarene (N3−H3n···O10 of 2.988(11) Å and N4−H4n···O9 of 2.83(2) Å; Figure 2b). This leaves two calixarene N−H groups free to form hydrogen bonds with carbonyl oxygen atoms of two neighboring molecules (N1−H1n···O8 of 2.883(6) Å and N2−H2n···O7 of 2.922(5) Å), leading to formation of chains along the crystallographic *b* axis (Figure 3).

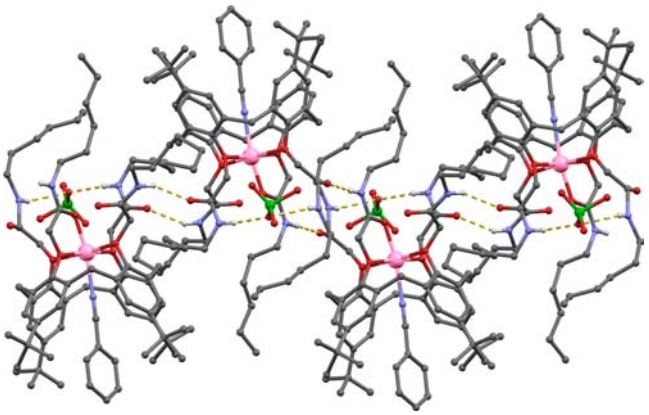

Figure 3. The hydrogen-bonded chains in the crystal structure of [Li**L**]ClO_4−PhCN.

Studies of Cation Complexation and Acetonitrile Inclusion in Benzonitrile. Complexation of calixarene **L** with lithium, sodium, and potassium cations in benzonitrile was studied by means of microcalorimetric titrations. The process of acetonitrile inclusion in the hydrophobic cone of these complexes was also investigated by this method.

The addition of $LiClO_4$ or $NaClO_4$ solution in PhCN to the solution of **L** resulted in negative enthalpy change. The stability constants of the complexes formed, along with the corresponding standard reaction enthalpies (Table 1), were computed by the nonlinear least-squares analysis of the calorimetric data.

Table 1. Thermodynamic Parameters for Complexation of Alkali Metal Cations with L in Benzonitrile at 25 °C Obtained by Microcalorimetry

cation	log K ± SE	($\Delta_r G°$ ± SE)/ kJ mol^{-1}	($\Delta_r H°$ ± SE)/ kJ mol^{-1}	($\Delta_r S°$ ± SE)/ J K^{-1} mol^{-1}
Li^+	6.17 ± 0.01	−35.24 ± 0.05	−8.9 ± 0.1	88.1 ± 0.4
Na^+	5.54 ± 0.01	−31.61 ± 0.04	−16.6 ± 0.1	50.4 ± 0.5
K^+	–[a]	–[a]	–[a]	–[a]

[a]No heat effects were observed upon addition of cation salt solution to ligand solution. SE = standard error of the mean (N = 3−5).

Standard reaction Gibbs energies and entropies were calculated from the above thermodynamic reaction quantities. As an example, titration data for the complexation of **L** with the lithium cation are shown in Figure 4 (those corresponding to the titration of **L** with Na^+ are given in Supporting Information, Figure S2). From the data presented in Table 1, it can be seen that the investigated calixarene derivative readily binds both lithium and sodium cations in benzonitrile. The titration of **L** with KSCN produced no significant heat effects, which could be a consequence of an isoenthalpic complexation process or low affinity of the ligand toward the potassium cation in benzonitrile.

Having obtained the stability constants of Li**L**$^+$ and Na**L**$^+$ complexes, it was possible to determine thermodynamic reaction quantities associated with the acetonitrile molecule inclusion into the calixarene basket of these species (Table 2). That was done by microcalorimetric titrations (Figure 5 and Supporting Information Figure S3) in which the solution of **L** with an excess of metal ion was titrated with the solution of acetonitrile in benzonitrile. According to the high affinity of **L** toward lithium and sodium ions in benzonitrile, the analytical calixarene−cation complex concentration could be safely approximated by the analytical concentration of **L**. The formation of acetonitrile adduct of both complexes is enthalpically favorable, whereas the standard reaction entropy for these processes is unfavorable. In addition to the exothermic process of acetonitrile inclusion in the Li**L**$^+$, an endothermic process taking place in the course of titration was also observed (Figure 5a). This process can be attributed to the endothermic mixing of acetonitrile and benzonitrile.

Ligand **L** binds Li^+ more strongly than Na^+ in benzonitrile (Table 1), whereas the opposite is true with acetonitrile as solvent.[4a] This interesting finding can be thermodynamically explained by analysis of the difference between standard transfer Gibbs energies of Li^+−**L** and Na^+−**L** complexes from acetonitrile to benzonitrile:

$$\Delta\Delta_t G°(M^+\text{–}\mathbf{L}, \text{MeCN} \rightarrow \text{PhCN}) = \Delta_r G°(Li^+\text{–}\mathbf{L}, \text{PhCN}) - \Delta_r G°(Na^+\text{–}\mathbf{L}, \text{PhCN}) - \Delta_r G°(Li\mathbf{L}MeCN^+, \text{MeCN}) + \Delta_r G°(Na\mathbf{L}MeCN^+, \text{MeCN}) + \Delta_t G°(Li^+, \text{MeCN} \rightarrow \text{PhCN}) - \Delta_t G°(Na^+, \text{MeCN} \rightarrow \text{PhCN}) \quad (1)$$

M^+−**L** denotes complex species with or without solvent molecule in the ligand cone, $\Delta_r G°(Li^+\text{–}\mathbf{L}, \text{PhCN})$ and $\Delta_r G°(Na^+\text{–}\mathbf{L}, \text{PhCN})$ are complexation Gibbs energies obtained in this work (Table 1), whereas the values $\Delta_r G°(Li\mathbf{L}MeCN^+, \text{MeCN}) + \Delta_r G°(Na\mathbf{L}MeCN^+, \text{MeCN})$ corresponding to formation of complex adducts in acetonitrile were determined earlier.[4a] The cation transfer Gibbs energies $\Delta_t G°(Li^+, \text{MeCN}\rightarrow\text{PhCN})$ and $\Delta_t G°(Na^+, \text{MeCN}\rightarrow\text{PhCN})$, based on Ph_4AsPh_4B convention, were taken from ref 23. The obtained value, $\Delta\Delta_t G°(M^+\text{–}\mathbf{L}, \text{MeCN}\rightarrow\text{PhCN}) = -10.3$ kJ mol^{-1}, indicates that the complexation of the lithium ion by **L** in benzonitrile is accompanied by favorable process(es) stabilizing the complex. This could be the inclusion of the benzonitrile molecule in the calixarene cone of Li**L**$^+$ complex (as evidenced in the solid state), which should then be less pronounced in the case of Na**L**$^+$. As an indication of larger affinity of the lithium complex toward the inclusion of benzonitrile can serve the difference between the standard reaction entropies for the inclusion of acetonitrile in the hydrophobic cavity of lithium and sodium complexes with **L** in benzonitrile. The MeCN molecule inclusion in PhCN is

dx.doi.org/10.1021/ic4019184 | *Inorg. Chem.* 2013, 52, 12702−12712

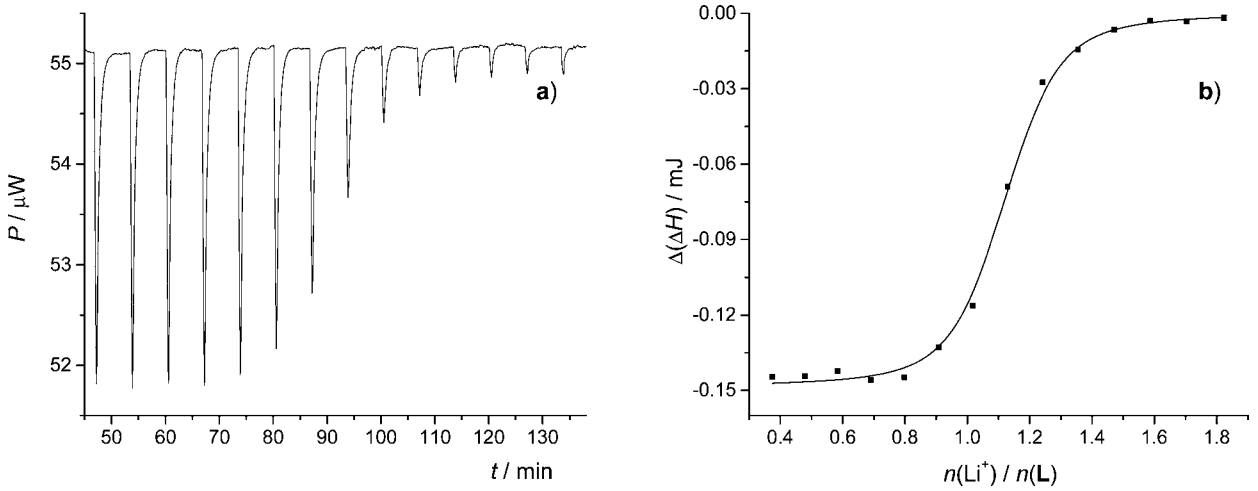

Figure 4. (a) Microcalorimetric titration of **L** ($c = 1.25 \times 10^{-4}$ mol dm^{-3}, $V = 1.4182$ mL) with $LiClO_4$ ($c = 1.18 \times 10^{-3}$ mol dm^{-3}) in benzonitrile; $t = 25$ °C. (b) Dependence of successive enthalpy change on $n(Li^+)/n(\mathbf{L})$ ratio. ■, experimental; −, calculated.

Table 2. Thermodynamic Parameters for the Inclusion of Acetonitrile in the Complexes of Li^+ and Na^+ Cations with L in Benzonitrile at 25 °C Obtained by Microcalorimetry[a]

ML^+	log K ± SE	$(\Delta_tG°$ ± SE)/ kJ mol^{-1}	$(\Delta_tH°$ ± SE)/ kJ mol^{-1}	$(\Delta_tS°$ ± SE)/ J K^{-1} mol^{-1}
Li**L**$^+$	0.62 ± 0.01	−3.56 ± 0.05	−20.3 ± 0.8	−56 ± 3
Na**L**$^+$	2.08 ± 0.02	−11.9 ± 0.1	−35.0 ± 0.9	−78 ± 3

[a]SE = standard error of the mean ($N = 3–5$).

entropically less unfavorable for Li**L**$^+$ than for Na**L**$^+$ (Table 2), which could be explained by taking into account possible substitution of the benzonitrile molecule in Li**L**$^+$ cone with acetonitrile. During the latter process, the overall number of free molecules in the solution remains constant, which in turn does not decrease translational entropy as would the inclusion of acetonitrile in an unoccupied cone.

To confirm additionally that the specific interaction of the benzonitrile molecule with the cone of Li**L**$^+$ has a dominant role in determining the relative difference of the Li^+−**L**/Na^+−**L** complex stabilities in the two solvents, we calculated the difference between the standard Gibbs energies of transfer of Li**L**MeCN$^+$ and Na**L**MeCN$^+$ species from acetonitrile to benzonitrile. The reason lies in the fact that this difference is affected only by the solvation of the complexes, and not by the inclusion of PhCN molecule, because the hydrophobic cavity of **L** is already occupied by MeCN. By combining the $\Delta\Delta_tG°(M^+–\mathbf{L}$, MeCN→PhCN) value (eq 1) and standard reaction Gibbs energies for the reaction of Li**L**$^+$ and Na**L**$^+$ with acetonitrile in benzonitrile, $\Delta_rG°$(Li**L**MeCN$^+$, PhCN) and $\Delta_rG°$(Na**L**MeCN$^+$, PhCN), respectively (Table 2), the mentioned difference in standard Gibbs energies of transfer can be obtained as:

$$\Delta\Delta_tG°(\mathbf{ML}\text{MeCN}^+, \text{MeCN} \rightarrow \text{PhCN}) = \Delta\Delta_tG°(M^+–\mathbf{L}, \text{MeCN} \rightarrow \text{PhCN}) + \Delta_rG°(\text{Li}\mathbf{L}\text{MeCN}^+, \text{PhCN}) - \Delta_rG°(\text{Na}\mathbf{L}\text{MeCN}^+, \text{PhCN}) \quad (2)$$

By comparing the obtained value of only −1.9 kJ mol^{-1} with $\Delta\Delta_tG°(M^+–\mathbf{L}$, MeCN→PhCN) = −10.3 kJ mol^{-1} (see above), it becomes clear that the relative difference in solvation of the complexes in the two solvents is of little importance, but the process mainly responsible for the fact that the thermodynamic stability of Li^+−**L** complex in PhCN is greater than that of

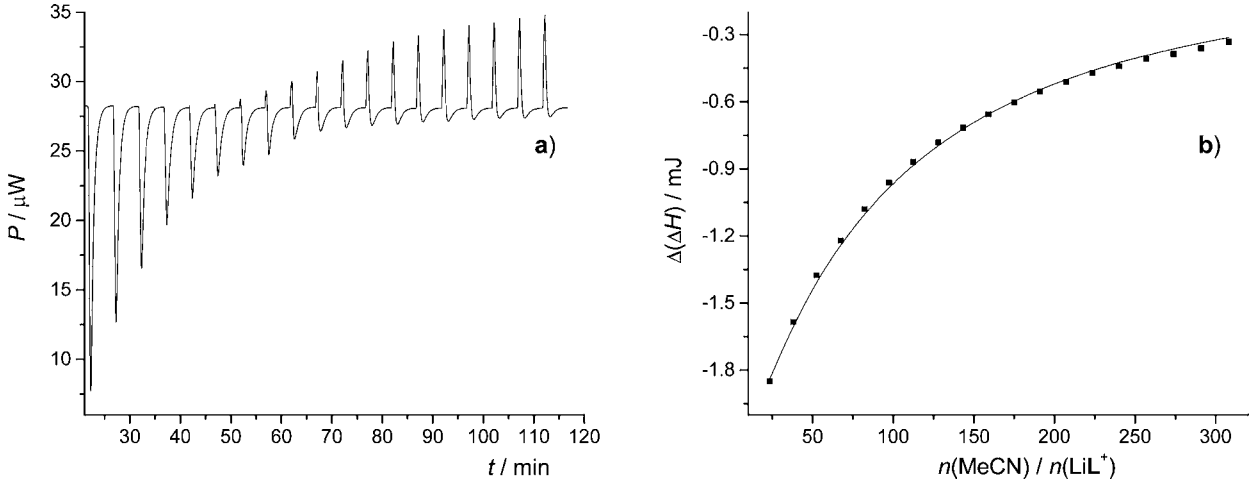

Figure 5. (a) Microcalorimetric titration of Li**L**$^+$ ($c = 1.13 \times 10^{-3}$ mol dm^{-3}, $V = 1.4182$ mL) with MeCN ($c = 1.50$ mol dm^{-3}) in benzonitrile; $t = 25$ °C. (b) Dependence of successive enthalpy change on $n(\text{MeCN})/n(\text{Li}\mathbf{L}^+)$ ratio. ■, experimental; −, calculated.

dx.doi.org/10.1021/ic4019184 | Inorg. Chem. 2013, 52, 12702−12712

Na^+−**L** species is the inclusion of PhCN molecule in the cone of the complexed **L**, which occurs to a larger extent in the case of Li**L**$^+$ as compared to Na**L**$^+$ complex.

Molecular dynamics simulations of free **L**, its lithium and sodium complexes, and their acetonitrile adducts in benzonitrile were performed. Throughout the simulation of the free macrocycle, no inclusion of the benzonitrile molecule in the calixarene hydrophobic basket was observed, and it remained all of the time in the shape of flattened cone. This shape was previously observed in the MD simulations of **L** in acetonitrile as well as in its solid-state structure.[4a] An intramolecular NH···O═C hydrogen-bond network was formed between the substituents at the lower rim, with an average of 2.3 such bonds present during simulation. In 50% of the structures where two or more H-bonds were formed, three-centered hydrogen bonds (two hydrogen atoms bound to one oxygen atom) were present (Figure S4, Supporting Information).

In the MD simulation of the Li**L**$^+$ complex, the metal cation was on average coordinated with 2.4 carbonyl oxygen atoms (Table S1, Supporting Information). The calixarene basket in this complex was also in a flattened cone conformation, although less flattened than in the case of free **L**. In the course of the simulations, the inclusion of the benzonitrile molecule in the hydrophobic cone of Li**L**$^+$ was observed. The solvent molecule was oriented either with the nitrile group pointed toward the bulk (Li**L**PhCN′$^+$, Figure 6a), or oppositely

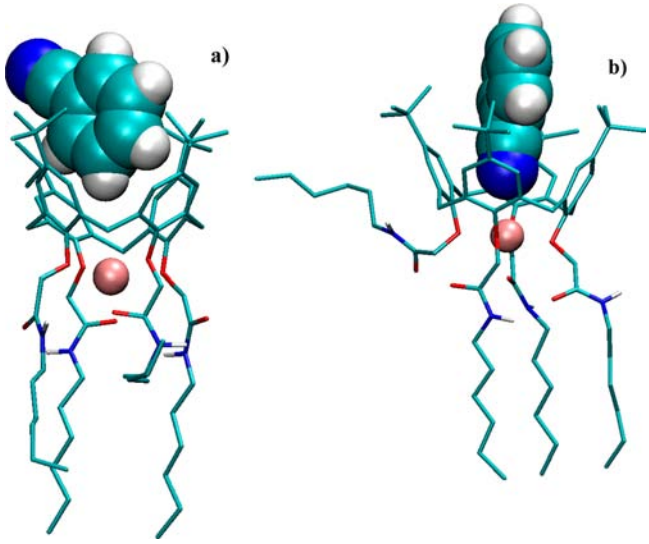

Figure 6. Molecular structure of (a) Li**L**PhCN′$^+$, 11.5 ns, and (b) Li**L**PhCN$^+$, 25.5 ns, after the beginning of molecular dynamics simulation in benzonitrile at 25 °C. Hydrogen atoms bound to carbon atoms of **L** have been omitted for clarity.

(Li**L**PhCN$^+$, Figure b). In the latter case, the nitrile group coordinated the metal cation in a fashion similar to that in the corresponding crystal structure (Figure 2), whereas the former resembled crystal structures with other noncoordinating aromatic molecules included in the calixarene cone.[24] The adduct Li**L**PhCN′$^+$ was observed in about 9% of total simulation time. This species exhibited the exchange of the solvent molecule in the hydrophobic basket, where 12 different PhCN molecules occupied the calixarene cone during simulation. The cone was more regular than in the case of the free ligand and Li**L**$^+$ complex, but it still remained somewhat flattened. The adduct Li**L**PhCN$^+$ proved to be much more stable than Li**L**PhCN′$^+$ and was observed in about 64% of simulation time. In addition, when the solvent molecule entered the hydrophobic cone of Li**L**$^+$ complex and coordinated the lithium cation, it remained there for the rest of simulation. The lithium cation was on average coordinated by four ether oxygen atoms, one carbonyl oxygen atom, and the nitrile group of benzonitrile, almost identically as in the solid-state structure (Figure 2). When coordinated by the PhCN nitrile group, Li^+ was shifted from the cation binding site formed by the lower-rim substituents toward the hydrophobic cavity of **L**. The distance of Li^+ from the geometric center of the ether oxygen atoms in Li**L**$^+$ complex was ∼1.1 Å, whereas in Li**L**PhCN$^+$ it amounted to only 0.2 Å (as compared to 0.002 Å in the crystal). The movement of the lithium cation decreased the number of ion-coordinating carbonyl oxygen atoms, which in turn made the interaction of Li^+ and **L** less favorable (−428 kJ mol^{-1} for Li**L**PhCN$^+$ as compared to −492 kJ mol^{-1} for Li**L**$^+$). However, that was compensated by the interaction energy of the specifically bound benzonitrile molecule with the lithium cation (−56 kJ mol^{-1}) as well as with the macrocycle **L** (−30 kJ mol^{-1}). Also, more intramolecular hydrogen bonds were present in the benzonitrile adduct of Li^+ complex with **L** (an average of 1.4 H-bonds) than in the complex without PhCN molecule in the cone (an average of 0.9 H-bonds). The lithium ion in Li**L**PhCN′$^+$ and Li**L**MeCN$^+$ species was coordinated in a fashion similar to that in Li**L**$^+$ complex, although the cation coordination number was larger in acetonitrile[4a] and benzonitrile adducts than in the solvent-free complex. The interaction energy of the lithium cation and **L** was the largest for Li**L**MeCN$^+$ adduct, whereas the average number of intramolecular hydrogen bonds in this species was the lowest among the Li^+−**L** complexes simulated. A rather strong binding of the lithium cation by carbonyl oxygen atom in Li**L**PhCN$^+$ can be evidenced by comparison of the distribution of angles between carbonyl group and Li^+ in different Li^+−**L** complexes in benzonitrile obtained by MD simulations (Figure S5, Supporting Information). The distribution corresponding to Li**L**PhCN$^+$ is much narrower, which indicates that the carbonyl group is preferably oriented toward the metal cation in this adduct. It is also noteworthy that the shape of the calixarene basket is closest to the regular cone in the Li**L**MeCN$^+$ and Li**L**PhCN$^+$ species.

In the MD simulations of Na**L**$^+$ complex in PhCN, the metal cation was coordinated with three carbonyl oxygen atoms (Table S2, Supporting Information). The solvent molecule inclusion in the calixarene basket was observed in 6% of simulation time, which was much less than in the case of Li**L**$^+$. As with the lithium complexes of **L**, two types of adduct were present: one in which the nitrile group of benzonitrile pointed toward the bulk (Na**L**PhCN′$^+$), and another where this group coordinated the metal cation (Na**L**PhCN$^+$). The former adduct was present in about 3% of simulation time, and exhibited a rather frequent solvent molecule exchange (32 different PhCN molecules occupied the cone during simulation). On the other hand, Na**L**PhCN$^+$ was formed on two occasions in the course of simulation with different solvent molecules. Although the sodium ion was coordinated by the nitrile group, contrary to the lithium complex, there was no significant displacement of the cation toward the calixarene cone. That caused only a slight decrease of the average Na^+ coordination number from 3.0 in Na**L**$^+$ to 2.85 in Na**L**PhCN$^+$. The described difference between sodium and lithium complexes most likely stems from the difference in cation sizes. Unlike Li^+ (r = 0.76 Å, coordination

dx.doi.org/10.1021/ic4019184 | Inorg. Chem. 2013, 52, 12702−12712

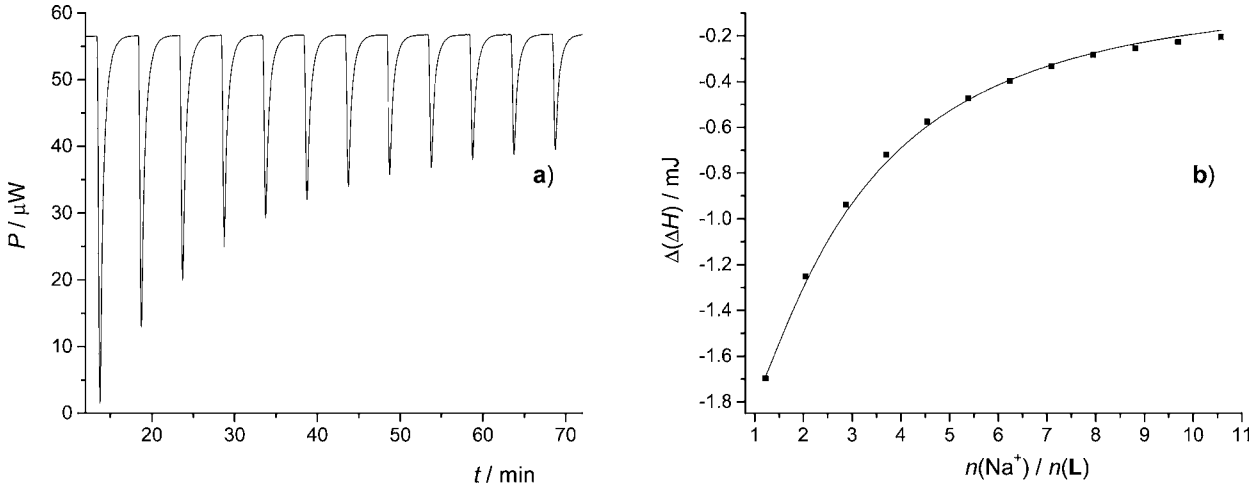

Figure 7. (a) Microcalorimetric titration of **L** ($c = 5.98 \times 10^{-4}$ mol dm^{-3}, $V = 1.4182$ mL) with $NaClO_4$ ($c = 6.86 \times 10^{-2}$ mol dm^{-3}) in methanol; $t = 25$ °C. (b) Dependence of successive enthalpy change on $n(Na^+)/n(\mathbf{L})$ ratio. ■, experimental; −, calculated.

Table 3. Thermodynamic Parameters for Complexation of Alkali Metal Cations with L in Methanol at 25 °C Obtained by Microcalorimetry, Spectrophotometry, and ^{1}H NMR Titrations

cation	log K ± SE	($\Delta_r G°$ ± SE)/kJ mol^{-1}	($\Delta_r H°$ ± SE)/kJ mol^{-1}	(($\Delta_r S°$ ± SE)/J K^{-1} mol^{-1})
Li^+	−[a,b]			
Na^+	2.74 ± 0.01[c]	−15.62 ± 0.06[c]	−13.6 ± 0.2[c]	6.8 ± 0.8[c]
	2.68 ± 0.04[d]			
	2.60[e]			
K^+	0.96 ± 0.05[f]			
Rb^+	−[b]			
Cs^+	−[b]			

[a]No heat effects were observed upon addition of cation salt solution to ligand solution. [b]No complexation was observed spectrophotometrically. [c]Determined by microcalorimetry. [d]Determined by spectrophotometry. [e]Determined by ^{1}H NMR spectroscopy. [f]Assessed by spectrophotometry. SE = standard error of the mean ($N = 3–5$).

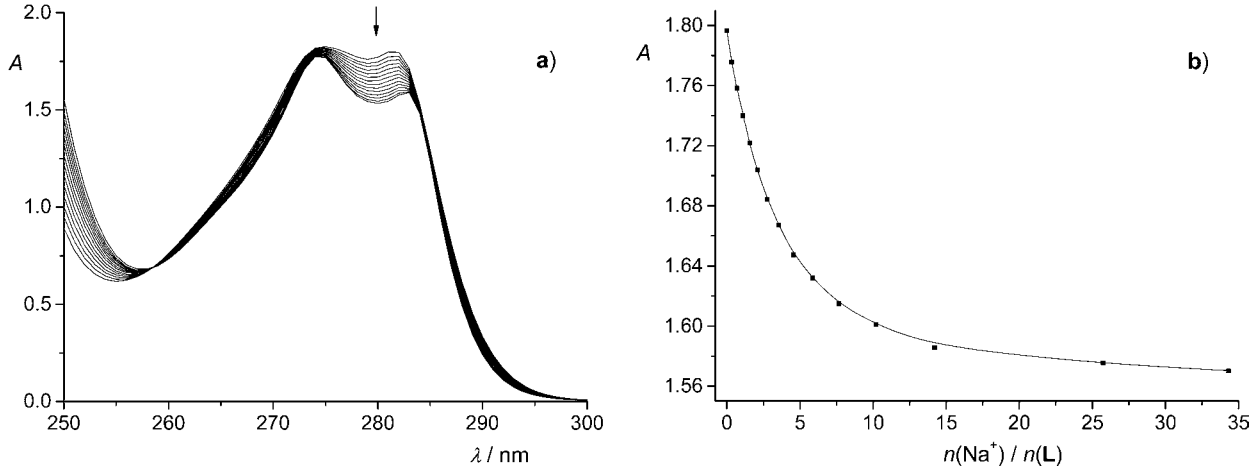

Figure 8. (a) Spectrophotometric titration of **L** ($c = 7.11 \times 10^{-4}$ mol dm^{-3}, $V_0 = 2$ mL) with $NaClO_4$ ($c = 3.49 \times 10^{-2}$ mol dm^{-3}) in methanol; $l = 1$ cm, $t = 25$ °C. The spectra are corrected for dilution. (b) Dependence of the absorbance at 282 nm on the $n(Na^+)/n(\mathbf{L})$ ratio. ■, experimental; −, calculated.

number 6),[25] sodium cation ($r = 1.02$ Å, coordination number 6)[25] is too big to be accommodated between the ether oxygen atoms of **L**. This is reflected in a much lower Na^+−PhCN interaction energy in $NaLPhCN^+$ species (−15 kJ mol^{-1}) as compared to that corresponding to Li^+−PhCN interaction (−56 kJ mol^{-1}, as stated above), which in turn leads to much more favorable inclusion of the benzonitrile molecule in LiL^+ than in NaL^+ complex. These findings corroborate the conclusions made on the basis of results obtained by calorimetric titrations.

Cation Complexation in Methanol. Complexation reactions of **L** with alkali-metal cations in methanol were also studied by experimental and computational methods. This solvent was chosen as a relatively polar one whose molecules can participate in hydrogen bonding, both as proton donors and as proton acceptors.

dx.doi.org/10.1021/ic4019184 | Inorg. Chem. 2013, 52, 12702−12712

The stability constant of NaL^+ complex in methanol and the corresponding standard complexation enthalpy and entropy were determined by microcalorimetric titrations (Figure 7). In these experiments, the heat of dilution of sodium perchlorate solution was comparable to the enthalpy change due to the reaction studied, and that considerably affected the quality of the obtained data. To reduce the heat of dilution, an inert electrolyte, Et_4NClO_4, was added to the ligand solution, whereby the electrolyte concentration was similar to that of the titrant. In that way, more reliable calorimetric data were obtained. The thermodynamic quantities obtained by processing these data (Table 3) show that, although the complexation reaction is both enthalpically and entropically favorable, the corresponding equilibrium constant is about 4 orders of magnitude lower in methanol than in acetonitrile.[4a]

Spectrophotometric titrations of **L** with the sodium cation in methanol were also conducted (Figure 8), and the stability constant of NaL^+ complex was determined by analyzing the collected spectra. By inspecting the data listed in Table 3, a very good agreement between the spectrophotometric and calorimetric values can be seen.

To gain more detailed insight into the complexation of Na^+ by **L** in methanol, ^{1}H NMR titration of **L** with Na^+ solution was carried out (Figure 9). The most significant changes in chemical shift were observed for calixarene Ar−H and *tert*-butyl protons. During titration, the ligand signals exhibited shifting and broadening, which indicated that the exchange kinetics of Na^+ + **L** complexation reaction was fast on the NMR time scale. The NaL^+ stability constant was determined from the dependence of the chemical shift of Ar−H and *tert*-butyl protons on the Na^+ cation concentration (Table 3), and is in good agreement with the corresponding values obtained by microcalorimetry and spectrophotometry.

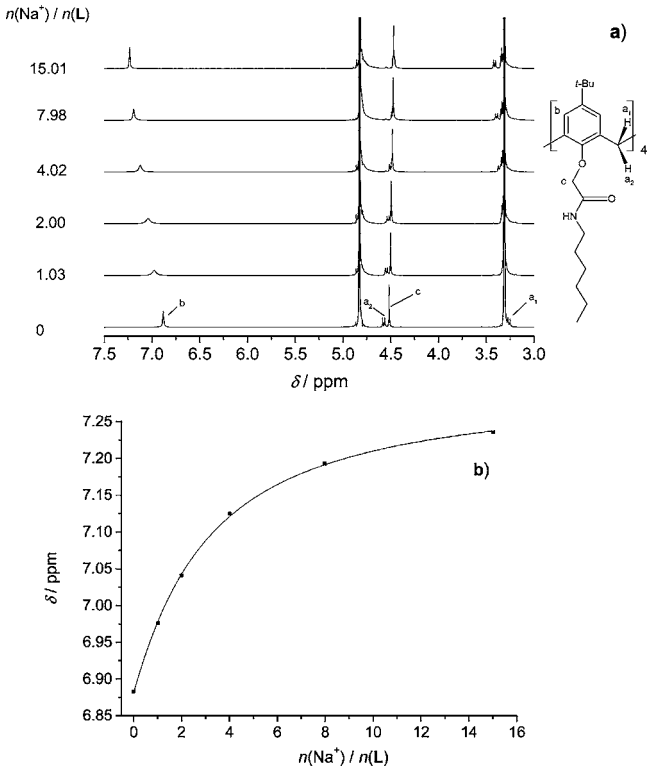

Figure 9. (a) ^{1}H NMR titration of **L** ($c = 9.72 \times 10^{-4}$ mol dm^{-3}) with $NaClO_4$ ($c = 3.84 \times 10^{-2}$ mol dm^{-3}) in CD_3OD; $t = 25$ °C. (b) Dependence of the chemical shift of Ar−H protons on the $n(Na^+)/n(L)$ ratio. ■, experimental; −, calculated.

As calix[4]arene−methanol adducts are well-known in the literature,[26] we have decided to investigate the MeOH molecule inclusion in hydrophobic cavities of **L** and NaL^+ by ^{1}H NMR titrations of these species with methanol in deuterated chloroform. The addition of methanol to the solution of **L** caused no significant shift in ligand signals (Figure S7, Supporting Information), apart from signals of amide protons. On the other hand, the addition of methanol to the solution of NaL^+ caused shifting of signals corresponding to Ar−H and *tert*-butyl protons of **L** (Figure S8, Supporting Information). The equilibrium constant for the inclusion of MeOH molecule in the NaL^+ complex in $CDCl_3$ ($\log K = 0.87 \pm 0.05$) was determined by processing the dependence of chemical shifts of **L** protons on methanol concentration.

For the sake of comparison, an analogous titration of NaL^+ with MeCN in $CDCl_3$ was carried out (Figure S9, Supporting Information). The logarithm of equilibrium constant of the reaction of acetonitrile molecule inclusion in the NaL^+ species obtained by processing the corresponding ^{1}H NMR data amounts to 1.46 ± 0.01, indicating that the binding of MeCN in chloroform is more favorable than that of MeOH (see below for more details).

The stability constant of KL^+ complex in methanol is too low to be accurately determined by means of microcalorimetric or spectrophotometric titration. Nevertheless, it was possible to assess the value of this constant from the results of spectrophotometric titrations of **L** with the potassium cation in methanol (Figure S10a, Supporting Information). Because of a low affinity of **L** toward the potassium cation in methanol, in these titrations the starting titrand solution was a mixture of calixarene and potassium chloride. The KCl concentration was slightly below its solubility. During titration, a certain volume of reaction mixture was removed from the measuring cell and replaced by the same volume of the ligand solution. In data analysis, the association of potassium and chloride ions was taken into account.[27] Although the agreement between the experimental and calculated absorbances was quite good (Figure S10b, Supporting Information), it should be noted that at the highest potassium ion concentration only about 20% of the ligand was in the form of KL^+ complex (Figure S10d, Supporting Information). That makes the reliability of the determined stability constant questionable.

Addition of Li^+, Rb^+, or Cs^+ chlorides into methanol calixarene solution produced no significant effect on the absorbance of **L**, indicating that no observable complexation took place. In accord with that, in the calorimetric titration of the ligand with solution of Li^+ salt, no measurable enthalpy changes were observed. For Rb^+ and Cs^+, the same conclusion was made previously for reactions in acetonitrile.[4a] On the other hand, the stability constant of the lithium complex with **L** in MeCN is rather high ($\log K = 6.04$).[4a] Such a huge difference between LiL^+ complex stabilities in the two solvents can be mainly accounted for by the quite stronger solvation of the lithium cation in methanol, as evidenced by Gibbs energy of transfer of Li^+ from MeCN to MeOH ($\Delta_t G = -25.9$ kJ mol^{-1}).[28]

The structure of calixarene **L** in methanol was also explored by molecular dynamics simulations in which the shape of the ligand basket resembled the one observed in acetonitrile and benzonitrile; that is, it adopted a flattened cone conformation.

dx.doi.org/10.1021/ic4019184 | Inorg. Chem. 2013, 52, 12702−12712

During simulations, an inclusion of the solvent molecule in the basket was observed. Upon that, the macrocycle hydrophobic cone became almost regular with C_4 symmetry (Figure S11, Supporting Information). In the structure of **L**MeOH adduct, the methyl group of the methanol molecule was oriented toward the calixarene lower rim, whereas the hydroxyl group pointed toward an aryl carbon atom (Figure S12, Supporting Information). The binding mode of the methanol molecule in the cone was similar to that found in crystal structures of different calixarene−methanol adducts.[26] In total, the **L**MeOH species was present during 63% of simulation time, and three different solvent molecules occupied the ligand basket. Thus, the molecular dynamics simulations indicated that in methanol, like in acetonitrile,[4a] ligand **L** existed in two forms, the one with the solvent molecule and the other without it. However, the lifetime of the **L**MeOH adduct was considerably shorter than that of **L**MeCN.[4a] In addition, the inclusion of MeOH molecule in **L** in methanol was less directly evidenced by ^{1}H NMR spectroscopy than was the case for MeCN adduct.[4a] The above findings lead to a conclusion that, although both MeCN and MeOH molecules specifically interact with **L**, the interaction with acetonitrile is more favorable, and therefore **L**MeCN species is more abundant in acetonitrile than **L**MeOH in methanol.

As in acetonitrile[4a] and benzonitrile, intramolecular hydrogen bonds in the structure of **L** were also found to form in methanol. In the case of free ligand, there were on average 2.1 such bonds. In 64% of the cases with two or more H-bonds present, a three-centered bond (two hydrogen atoms bound to one oxygen atom) was formed, as in the crystal structures of the free ligand.[4a] For the **L**MeOH adduct, the number of intramolecular hydrogen bonds was lower than that for free **L**, with an average of 1.3 such bonds present. When two or more hydrogen bonds were formed, in 27% of the cases a three-centered H-bond was present (Figure S12, Supporting Information).

In the molecular dynamics simulations of Na**L**$^+$ and K**L**$^+$ complexes in methanol, an inclusion of MeOH molecule in the calixarene basket was also observed (Figure 10). This process resulted in rigidification of the calixarene basket, which became more regular than in the solvent-free complex, and that was reflected in an increase of the cation coordination number. The structural features of the Na**L**MeOH$^+$ and K**L**MeOH$^+$ adducts were found to be similar to those of Na**L**MeCN$^+$ and K**L**MeCN$^+$.[4a] No significant difference was observed between the average numbers of intramolecular hydrogen bonds in these species. The same holds for the number of carbonyl oxygen atoms coordinating the metal cation and the cation−ligand interaction energies (Table S3, Supporting Information). However, despite the above similarities, the inclusion of MeCN molecule in the ligand hydrophobic cavity in acetonitrile solutions of the complexes seems to be appreciably more favorable than that of MeOH molecule in methanol. This can be concluded by taking into account that a considerably larger number of solvent molecules entered and left the ligand hydrophobic cone in the course of simulations of methanol solutions. In addition, although both complexes in MeOH predominantly existed in the form of solvent adducts (Table S3, Supporting Information), the simulation time in which calixarene cone was without the solvent molecule was much longer than that found by the MD simulations of the corresponding acetonitrile solutions.[4a]

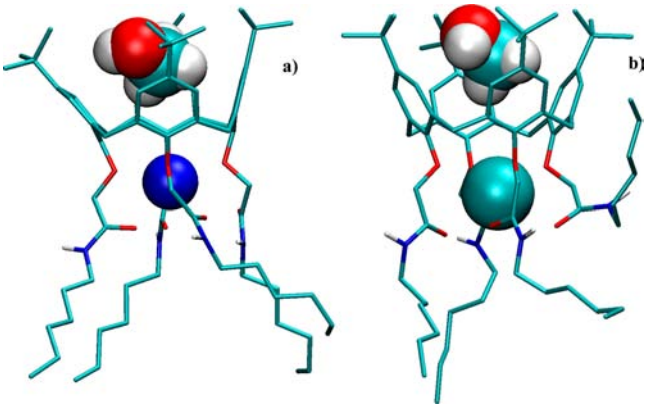

Figure 10. Molecular structure of (a) Na**L**MeOH$^+$, 30 ns, and (b) K**L**MeOH$^+$, 35 ns, after the beginning of molecular dynamics simulation in methanol at 25 °C. Hydrogen atoms bound to carbon atoms of **L** have been omitted for clarity.

To get more detailed thermodynamical information about the solvent effect on the reactions studied, an effort was made to determine the values of standard Gibbs energies of solution of **L** in acetonitrile, benzonitrile, and methanol. For that reason, the solubilities of the ligand in MeCN and MeOH were measured (Table 4). In the case of PhCN, we were unable to determine the solubility of **L** because of gelation of concentrated solution. Standard solution Gibbs energies for methanol and acetonitrile as solvents were calculated from the solubility data using equation:

Table 4. Solubilities and Derived Standard Solution Gibbs Energies of L in Acetonitrile and Methanol at 25 °C

solvent	$10^4 \times s$/mol dm^{-3}	$\Delta_{sol}G°$/kJ mol^{-1}
acetonitrile	4.96	19.01
methanol	18.7	15.60

$$\Delta_{sol}G° = -RT \ln K° = -RT \ln(\gamma_L s/c°) \approx -RT \ln(s/c°) \quad (3)$$

where s denotes solubility, $c°$ = 1 mol dm^{-3} is standard concentration, and γ_L stands for the activity coefficient of the ligand, which is assumed to be close to unity. The obtained values are reported in Table 4 and were used to calculate transfer Gibbs energies of Na**L**$^+$ and K**L**$^+$ complexes from MeOH to MeCN (Scheme 1) by the following equation:

$$\Delta_tG°(\mathrm{ML}^+, \mathrm{MeOH} \rightarrow \mathrm{MeCN}) = \Delta_tG°(\mathrm{M}^+, \mathrm{MeOH} \rightarrow \mathrm{MeCN}) + \Delta_tG°(\mathbf{L}, (\mathrm{MeOH} \rightarrow \mathrm{MeCN}) + \Delta_rG°(\mathrm{MeCN}) - \Delta_rG°(\mathrm{MeOH}) \quad (4)$$

Indexes t and r denote transfer and complexation reaction, respectively.

The $\Delta_tG°(M^+, MeOH→MeCN)$ values for Na^+ and K^+ were calculated by combining the Gibbs energies of transfer of cations from water to methanol or acetonitrile based on Ph_4AsPh_4B convention[28] ($\Delta_tG°(M^+, MeOH→MeCN) = \Delta_tG°(M^+, H_2O→MeCN) - \Delta_tG°(M^+, H_2O→MeOH)$).

Even though the investigated calixarene is somewhat more soluble in methanol than in acetonitrile, the value of the Gibbs energy of its transfer from MeOH to MeCN is relatively low (3.28 kJ mol^{-1}). This suggests that the difference in solvation of the ligand is not predominant in determining the considerable difference in thermodynamic stabilities of the metal ion

dx.doi.org/10.1021/ic4019184 | Inorg. Chem. 2013, 52, 12702−12712

Scheme 1. Thermodynamic Cycles for Complexation of Na^+ and K^+ with L in Methanol and Acetonitrile Expressed in Terms of Gibbs Energies

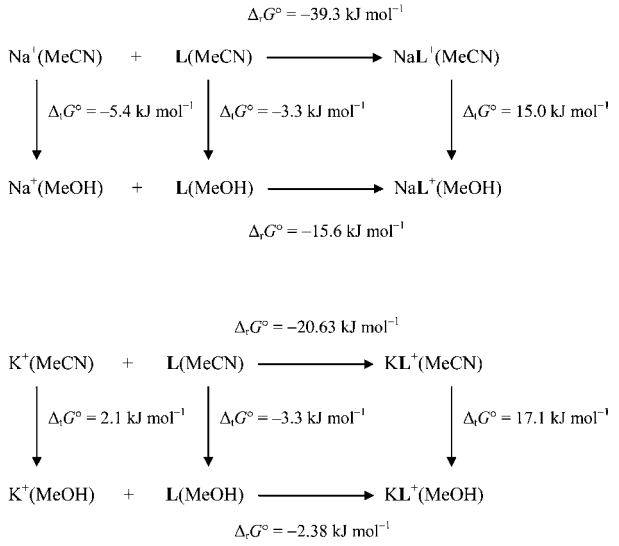

complexes in the two solvents. Therefore, apart from cation solvation (Na^+ is somewhat better solvated in MeOH than in MeCN, whereas the opposite holds for K^+, Scheme 1), obviously that of the complex species should be regarded as important. Indeed, the $\Delta_tG°$ values given in thermodynamic cycles presented in Scheme 1 show the transfer of both NaL^+ and KL^+ from methanol to acetonitrile to be quite favorable. It follows that solvation-based stabilization of the complexes in MeCN relative to MeOH is the decisive factor responsible for the higher stabilities of the complexes in the former solvent. According to our previous findings[3b,4a] and the present results, this can be accounted for by the fact that favorable inclusion of the solvent molecule in the hydrophobic cavity of the complexed ligand is more pronounced in acetonitrile than in methanol. That presents another good example of the impact of specific solvent–solute interactions on the stability of macrocycle complexes.

CONCLUSION

The presented results clearly show how remarkable is the role of solvent in determining the equilibria of complexation reactions. To get a detailed insight into the process of binding of alkali-metal cations with calixarene derivative **L** in various solvents, comprehensive solution and solid-state structural, thermodynamic, and computational studies have been carried out. The stability constants of the complexes of **L** with alkali-metal cations were determined, as were the corresponding reaction enthalpies and entropies. Both enthalpic and entropic contributions were found to be favorable for the reactions examined. However, thermodynamic stabilities of the ML^+ complexes were rather solvent dependent (stability decreased in the solvent order: MeCN > PhCN > MeOH), which could be accounted for by considering the differences in the solvation of the cations as well as free and complexed ligand. With this respect, the specific solvent–solute interaction, that is, inclusion of the solvent molecule in the calixarene hydrophobic cavity, was proven to be quite important. Interestingly, macrocycle **L** was shown to be a better binder of Li^+ as compared to Na^+ in PhCN, which was in contrast to MeCN as a solvent. That could be explained by the inclusion of the PhCN molecule into the ligand hydrophobic cone of the LiL^+ complex observed in the solid state. More precisely, in the molecular structure of the lithium complex of **L** determined by single-crystal X-ray diffraction analysis, the PhCN molecule bound in the calixarene cone was found to coordinate the Li^+ cation by its nitrile group. This favorable nitrile compound–alkali-metal cation interaction in the calixarene complex was to our knowledge observed for the first time. The experimental results were supported by those obtained by MD simulations.

ASSOCIATED CONTENT

Supporting Information

X-ray crystallographic data in CIF format; results of the Cambridge Structural Database search for metal complexes of calix[4]arenes where an acetonitrile molecule included in the calixarene cone is coordinatively bound to the central ion; additional results of microcalorimetric, spectrophotometric, and ^{1}H NMR titrations; and results of MD simulations. This material is available free of charge via the Internet at http://pubs.acs.org.

AUTHOR INFORMATION

Corresponding Author

*E-mail: vtomisic@chem.pmf.hr.

Notes

The authors declare no competing financial interest.

ACKNOWLEDGMENTS

This work was supported by the Ministry of Science, Education, and Sports of the Republic of Croatia (projects 119-1191342-2960, 119-1193079-3069, and 098-0982904-2912). Computational resources provided by the Croatian National Grid Infrastructure (www.cro-ngi.hr) at Zagreb University Computing Centre (Srce) were used for this publication.

REFERENCES

(1) (a) Gutsche, C. D. *Calixarenes: An Introduction*, 2nd ed.; The Royal Society of Chemistry: Cambridge, UK, 2008. (b) *Calixarenes 2001*; Asfari, Z., Böhmer, V., Harrowfield, J., Vicens, J., Eds.; Kluwer Academic Publishers: Dordrecht, Netherlands, 2001. (c) *Calixarenes in the Nanoworld*; Vicens, J., Harrowfield, J., Eds.; Springer: Dordrecht, Netherlands, 2001. (d) Danil de Namor, A. F.; Cleverley, R. M.; Zapata-Ormachea, M. L. *Chem. Rev.* **1998**, *98*, 2495–2526. (e) Böhmer, V. *Angew. Chem., Int. Ed. Engl.* **1995**, *34*, 713–745.

(2) (a) Sliwa, W.; Girek, T. *J. Inclusion Phenom. Macrocyclic Chem.* **2010**, *66*, 15–41. (b) Schühle, D. T.; Peters, J. A.; Schatz, J. *Coord. Chem. Rev.* **2011**, *255*, 2727–2745. (c) Mokhtari, B.; Pourabdollah, K.; Dalali, N. *J. Inclusion Phenom. Macrocyclic Chem.* **2010**, *69*, 1–55. (d) Ludwig, R.; Dzung, N. T. K. *Sensors* **2002**, *2*, 397–416. (e) Creaven, B. S.; Donlon, D. F.; McGinley, J. *Coord. Chem. Rev.* **2009**, *253*, 893–962.

(3) (a) Tomišić, V.; Galić, N.; Bertoša, B.; Frkanec, L.; Simeon, V.; Žinić, M. *J. Inclusion Phenom. Macrocyclic Chem.* **2005**, *53*, 263–268. (b) Požar, J.; Preočanin, T.; Frkanec, L.; Tomišić, V. *J. Solution Chem.* **2010**, *39*, 835–848. (c) Danil de Namor, A. F.; Hutcherson, R. G.; Velarde, F. J. S.; Zapata-Ormachea, M. L.; Salazar, L. E. P.; Jammaz, I.; Rawi, N. *Pure Appl. Chem.* **1998**, *70*, 769–778. (d) Danil de Namor, A. F. In *Calixarenes 2001*; Asfari, Z., Böhmer, V., Harrowfield, J., Vicens, J., Eds.; Kluwer Academic Publishers: Dordrecht, Netherlands, 2001; pp 346–364. (e) Arnaud-Neu, F.; McKervey, M. A.; Schwing-Weill, M.-J. In *Calixarenes 2001*; Asfari, Z., Böhmer, V., Harrowfield, J., Vicens, J., Eds.; Kluwer Academic Publishers: Dordrecht, Netherlands, 2001; pp 385–406. (f) Danil de Namor, A. F.; Matsufuji-Yasuda, T. T.; Zegarra-Fernandez, K.; Webb, O. A.; El Gamouz, A. *Croat. Chem. Acta* **2013**, *86*, 1–19.

(4) (a) Horvat, G.; Stilinović, V.; Hrenar, T.; Kaitner, B.; Frkanec, L.; Tomišić, V. *Inorg. Chem.* **2012**, *51*, 6264−6278. (b) Danil de Namor, A. F.; de Sueros, N. A.; McKervey, M. A.; Barrett, G.; Neu, F. A.; Schwing-Weill, M. J. *J. Chem. Soc., Chem. Commun.* **1991**, 1546−1548. (c) Danil de Namor, A. F.; Chahine, S.; Castellano, E. E.; Piro, O. E. *J. Phys. Chem. A* **2005**, *109*, 6743−6751. (d) Danil de Namor, A. F.; Gil, E.; Tanco, M. A. L.; Tanaka, D. A. P.; Salazar, L. E. P.; Schulz, R. A.; Wang, J. *J. Phys. Chem.* **1995**, *99*, 16781−16785. (e) Danil de Namor, A. F.; Zapata-Ormachea, M. L.; Hutcherson, R. G. *J. Phys. Chem. B* **1999**, *103*, 366−371. (f) Danil de Namor, A. F.; Chahine, S.; Kowalska, D.; Castellano, E. E.; Piro, O. E. *J. Am. Chem. Soc.* **2002**, *124*, 12824−12836. (g) Danil De Namor, A. F.; Aparicio-Aragon, W. B.; Goitia, M. T.; Casal, A. R. *Supramol. Chem.* **2004**, *16*, 423−433. (h) Požar, J.; Horvat, G.; Čalogović, M.; Galić, N.; Frkanec, L.; Tomišić, V. *Croat. Chem. Acta* **2012**, *85*, 541−552.

(5) (a) Nomura, E.; Takagaki, M.; Nakaoka, C.; Uchida, M.; Taniguchi, H. *J. Org. Chem.* **1999**, *64*, 3151−3156. (b) Frkanec, L.; Višnjevac, A.; Kojić-Prodić, B.; Žinić, M. *Chem.-Eur. J.* **2000**, *6*, 442−453. (c) Mareque Rivas, J. C.; Schwalbe, H.; Lippard, S. J. *Proc. Natl. Acad. Sci. U.S.A.* **2001**, *98*, 9478−9483. (d) Tomišić, V.; Galić, N.; Bertoša, B.; Frkanec, L.; Simeon, V.; Žinić, M. *J. Inclusion Phenom. Macrocyclic Chem.* **2005**, *53*, 263−268. (f) Galić, N.; Burić, N.; Tomaš, R.; Frkanec, L.; Tomišić, V. *Supramol. Chem.* **2011**, *23*, 389−397.

(6) (a) Gampp, H.; Maeder, M.; Meyer, C. J.; Zuberbühler, A. D. *Talanta* **1985**, *32*, 95−101. (b) Gampp, H.; Maeder, M.; Meyer, C. J.; Zuberbühler, A. D. *Talanta* **1985**, *32*, 257−264. (c) Maeder, M.; Zuberbühler, A. D. *Anal. Chem.* **1990**, *62*, 2220−2224.

(7) (a) Frassineti, C.; Ghelli, S.; Gans, P.; Sabatini, A.; Moruzzi, M. S.; Vacca, A. *Anal. Biochem.* **1995**, *231*, 374−382. (b) Frassineti, C.; Alderighi, L.; Gans, P.; Sabatini, A.; Vacca, A.; Ghelli, S. *Anal. Bioanal. Chem.* **2003**, *376*, 1041−1052.

(8) Tellinghuisen, J. *J. Phys. Chem. B* **2007**, *111*, 11531−11537.

(9) Oxford Diffraction. *CrysAlis CCD and CrysAlis RED, version 1.170*; Oxford Diffraction Ltd.: Wroclaw, Poland, 2003.

(10) Sheldrick, G. M. *Acta Crystallogr., Sect. A: Found. Crystallogr.* **2008**, *64*, 112−122.

(11) Farrugia, L. J. *J. Appl. Crystallogr.* **1999**, *32*, 837−838.

(12) (a) Spek, A. L. *PLATON, version of July 1999*; Utrecht University: The Netherlands, 1999. (b) Van der Sluis, P.; Spek, A. L. *Acta Crystallogr., Sect. A: Found. Crystallogr.* **1990**, *46*, 194−201.

(13) Hess, B.; Kutzner, C.; van der Spoel, D.; Lindahl, E. *J. Chem. Theory Comput.* **2008**, *4*, 435−447.

(14) Jorgensen, W. L.; Maxwell, D. S.; Tirado-Rives, J. *J. Am. Chem. Soc.* **1996**, *118*, 11225−11236.

(15) Swope, W. C.; Andersen, H. C.; Berens, P. H.; Wilson, K. R. *J. Chem. Phys.* **1982**, *76*, 637−649.

(16) (a) Darden, T.; York, D.; Pedersen, L. *J. Chem. Phys.* **1993**, *98*, 10089−10092. (b) Essmann, U.; Perera, L.; Berkowitz, M. L.; Darden, T.; Lee, H.; Pedersen, L. G. *J. Chem. Phys.* **1995**, *103*, 8577−8593.

(17) (a) Nosé, S. *Mol. Phys.* **1984**, *52*, 255−268. (b) Hoover, W. *Phys. Rev. A* **1985**, *31*, 1695−1697.

(18) Martyna, G. J.; Tuckerman, M. E.; Tobias, D. J.; Klein, M. L. *Mol. Phys.* **1996**, *87*, 1117−1157.

(19) Humphrey, W.; Dalke, A.; Schulten, K. *J. Mol. Graphics* **1996**, *14*, 33−38.

(20) Allen, F. H. *Acta Crystallogr., Sect. B: Struct. Sci.* **2002**, *58*, 380−388.

(21) (a) Giannini, L.; Solari, E.; Zanotti-Gerosa, A.; Floriani, C.; Chiesi-Villa, A.; Rizzoli, C. *Angew. Chem., Int. Ed. Engl.* **1997**, *36*, 753−754. (b) Floriani, C. *Chem.-Eur. J.* **1999**, *5*, 19−23. (c) Gueneau, E. D.; Fromm, K. M.; Goesmann, H. *Chem.-Eur. J.* **2003**, *9*, 509−514.

(22) Ugozzoli, F.; Andreetti, G. D. *J. Inclusion Phenom.* **1992**, *13*, 337−348.

(23) Danil de Namor, A. F.; Rawi, N. Al; Piro, O. E.; Castellano, E. E.; Gil, E. *J. Phys. Chem. B* **2002**, *106*, 779−787.

(24) (a) Giannini, L.; Caselli, A.; Solari, E.; Floriani, C.; Chiesi-Villa, A.; Rizzoli, C.; Re, N.; Sgamellotti, A. *J. Am. Chem. Soc.* **1997**, *119*, 9709−9719. (b) Giannini, L.; Solari, E.; Dovesi, S.; Floriani, C.; Re, N.; Chiesi-Villa, A.; Rizzoli, C. *J. Am. Chem. Soc.* **1999**, *121*, 2784−2796. (c) Guillemot, G.; Solari, E.; Floriani, C.; Rizzoli, C. *Organometallics* **2001**, *20*, 607−615. (d) Dubberley, S. R.; Friedrich, A.; Willman, D. A.; Mountford, P.; Radius, U. *Chem.-Eur. J.* **2003**, *9*, 3634−3654. (e) Salmon, L.; Thuéry, P.; Asfari, Z.; Ephritikhine, M. *Dalton Trans.* **2006**, 3006−3014.

(25) *CRC Handbook of Chemistry and Physics*, 87th ed.; Lide, D. R., Ed.; CRC Press: Boca Raton, FL, 2006; p 11−12.

(26) (a) Camiolo, S.; Galea, P. A.; Light, M. E. *Supramol. Chem.* **2001**, *13*, 613−618. (b) Stumpf, S.; Goretzki, G.; Gloe, K.; Gloe, K.; Seichter, W.; Weber, E.; Bats, J. A. N. W.; Chemie, O.; Frankfurt, J. W. G. U.; Frankfurt, D. *J. Inclusion Phenom. Macrocyclic Chem.* **2003**, *45*, 225−233. (c) Liua, Y.; Lia, Z.; Guoa, D.-S. *Supramol. Chem.* **2009**, *21*, 465−472.

(27) Grunwald, E.; Brown, C. D. *J. Phys. Chem.* **1982**, *86*, 182−184.

(28) Burgess, J. *Metal Ions in Solution*; Ellis Horwood: Chichester, 1978.